NASA Technical Memorandum 85892

Hover Test of a Full-Scale Hingeless Helicopter Rotor: Aeroelastic Stability, Performance, and Loads Data

Randall L. Peterson and William Warmbrodt

January 1984

NASA
National Aeronautics and
Space Administration

ENTER:

SELECT ER6 SE104: TERM NOT IN DICTIONARY

11 45 45 AU/PETERSON, R. L.

12 1 1 RN/NASA-TM-85892

DISPLAY 12/6/1

84N18190*# ISSUE 9 PAGE 1255 CATEGORY 5 RPT#: NASA-TM-85892 A-9573

NAS 1.15:85892 84/01/00 52 PAGES UNCLASSIFIED DOCUMENT

UTTL: Hover test of a full-scale hingeless helicopter rotor: Aeroelastic stability, performance and loads data --- wind tunnel tests

AUTH: A/PETERSON, R. L.; B/WARMBRODT, W.

CORP: National Aeronautics and Space Administration. Ames Research Center, Moffett Field, Calif. AVAIL.NTIS SAP: HC A04/MF A01

MAJS: /*AEROELASTICITY/*DYNAMIC STABILITY/*HELICOPTER DESIGN/*HOVERING/*RIGID ROTORS/*WIND TUNNEL TESTS

MINS: / LOADS (FORCES)/ ROTARY WINGS/ ROTOR SPEED/ TABLES (DATA)/ THRUST

ABA: Author

NASA Technical Memorandum 85892

Hover Test of a Full-Scale Hingeless Helicopter Rotor: Aeroelastic Stability, Performance, and Loads Data

Randall L. Peterson
William Warmbrodt, Ames Research Center, Moffett Field, California

National Aeronautics and
Space Administration

Ames Research Center
Moffett Field, California 94035

TABLE OF CONTENTS

NOMENCLATURE

A1,B1	coefficients in the representation of rotor blade cyclic pitch, $-A1 \cos(\psi + 10°) - B1 \sin(\psi + 10°)$, deg
a_1, b_1	coefficients of $\cos \psi$ and $\sin \psi$ in Fourier expansion of measurement signal, respectively
CLR/S	rotor lift coefficient, positive vertical, rotor lift/$\rho S(\Omega R)^2$
CMX/S	rotor rolling moment coefficient, positive advancing side of rotor disk down, rotor rolling moment/$\rho S(\Omega R)^2 R$
CMY/S	rotor pitching moment coefficient, positive leading side of rotor disk up, rotor pitching moment/$\rho S(\Omega R)^2 R$
CMZ/S	rotor yawing moment coefficient, positive opposing direction of rotation, rotor yawing moment/$\rho S(\Omega R)^2 R$
CP/S	rotor power coefficient, rotor power/$\rho S(\Omega R)^3$
CPO/S	non-ideal rotor power coefficient, CPO/S = CP/S - CQ/S + CQO/S
CQ/S	rotor torque coefficient, rotor torque/$\rho \pi R^3 (\Omega R)^2$
CQO/S	non-ideal rotor torque coefficient, CQO/S = $(1/\sqrt{2})(CLR/S)^{3/2}(S/\pi R^2)^{1/2}$
C_T/σ,CT/S	rotor thrust coefficient, positive vertical thrust
CXR/S	rotor propulsive force coefficient, positive toward leading side of rotor disk, -drag/$\rho S(\Omega R)^2$
CYR/S	rotor side force coefficient, positive toward advancing side of rotor disk, rotor side force/$\rho S(\Omega R)^2$
c	speed of sound, m/sec
c	constant blade chord, m
N	total number of blades
OMEGA*R,ΩR	rotor blade tip speed, m/sec
R	rotor radius, m
RHO,ρ	air density, kg/m^3
rpm	rotor rotational speed, rev/min
S	reference area, S = NcR, m^2
SIGMA	damping decay coefficient, sec^{-1}

T 1/2	time to half amplitude, sec
THETA,θ	collective pitching setting at 0.7R, deg
TIPM	rotor rotational Mach number, $\Omega R/c$
VKNOTS,V	free-stream velocity, knots
ZETA,ζ	fixed system percent critical damping coefficient
σ	decay coefficient, sec^{-1}; rotor solidity, $S/\pi R^2$
ψ	rotor blade azimuth angle measured from fuselage tail centerline in direction of rotation, deg
Ω	rotor rotational speed, rad/sec
ω_ζ	fundamental rotating inplane bending frequency, rad/sec
ω_S	support motion frequency, Hz

SUMMARY

A hover test of a full-scale, hingeless rotor system was conducted in the NASA Ames 40- by 80-Foot Wind Tunnel. The rotor was tested on the Ames Rotor Test Apparatus (RTA). Rotor aeroelastic stability, performance, and loads at various rotational speeds and thrust coefficients were investigated. The primary objective was to determine the inplane stability characteristics of the rotor system. Rotor inplane damping data were obtained for operation between 350 and 425 rpm (design speed), and for thrust coefficients (C_T/σ) between 0.0 and 0.12. The rotor was stable for all conditions tested. At constant rotor rotational speed, a minimum inplane damping level was obtained at approximately $C_T/\sigma = 0.02$. At constant rotor lift, a minimum in rotor inplane damping was measured at 400 rpm.

INTRODUCTION

A full-scale BO-105 helicopter rotor system was tested in hover in the NASA Ames 40- by 80-Foot Wind Tunnel (fig. 1) to measure rotor aeroelastic stability, performance, and loads at various rotational speeds and thrust coefficients. This report presents the rotor aeroelastic stability, performance, and loads data, and the resultant vibration levels in the rotor test apparatus obtained from that test. The rotor hardware and test procedures are described. Rotor performance data are given in appendix A. Aeroelastic stability results are discussed, and the data are presented in appendix B. Rotor loads data for hover flight test conditions are tabulated in appendix C. The resultant vibration levels in the rotor test apparatus are presented in appendix D.

TEST HARDWARE

The BO-105 helicopter rotor system is a four-bladed, soft inplane ($\omega_\zeta < \Omega$) rotor with constant chord (0.27 m), -8° linear twist, and a NACA 23012 airfoil. The rotor radius is 4.91 m. The rotor hub has 2.5° of built-in coning and zero droop or sweep of the blade outboard of the pitch bearing (fig. 2). Additional data on the rotor system are listed in table 1, and in references 1 and 2. Calculated rotating coupled bending and uncoupled torsion frequencies at the design tip speed 218 m/sec (425 rpm) are presented in table 2 (ref. 2).

The rotor was installed on the Ames RTA for the test. This apparatus is a special purpose drive-and-support system for operating helicopter rotors in the 40- by 80-Foot Wind Tunnel. It houses two electric drive motors, the hydraulic servo actuators of the primary control system, and a dynamic control system which is capable of introducing dynamic perturbations to the nonrotating swashplate (collective and tilt), at frequencies up to 30 Hz. This system was used during testing to excite the rotor at its fundamental inplane-bending frequency for stability

measurements. The support system dynamic characteristics determined in a shake test performed immediately prior to this test are presented in table 3.

The rotor hardware, upper rotor controls, and the rotor test apparatus were instrumented to measure blade, pitch link, nonrotating swashplate, rotor shaft, and module moments, forces and vibrations. A complete list of rotor/module instrumentation is given in tables 4 and 5. Blade pitch was measured indirectly by measuring the positions of the three nonrotating control actuators. The positions of the three actuators gave a measure of swashplate tilt and, consequently, blade pitch. These measurements were made statically (nonrotating) and calibrated throughout the entire range of anticipated pitch control positions. The blade pitch settings presented herein are referenced to radial station 0.7R.

TESTING PROCEDURES

All testing was performed in simulated hover conditions. Prior to beginning a data acquisition run, the shaft tilt was set to -10°. Test conditions were established by setting rotor rotational speed and rotor thrust (C_T/σ). All testing was done at a shaft tilt of -10° with the wind tunnel access doors and exhaust louvers open. This was done in an attempt to reduce air flow recirculation and ground effect within the test section as the vane set in front of the drive section was in the closed position. Cyclic pitch was used to null any once-per-revolution flapping as measured using a resolved flapwise bending moment signal from the instrumented blade at 0.10R station. Longitudinal and lateral cyclic pitch inputs on the order of ±0.2° were required to null this once-per-revolution flapping. When the desired rotor rotational speed and thrust coefficient were reached, a data point was then taken for performance and steady-state dynamic data.

After obtaining performance and loads data, aeroelastic stability data were taken. The dynamic control system was used to oscillate the rotor cyclic pitch at the rotor regressing inplane bending frequency ($\Omega - \omega_\zeta$). A chordwise bending moment signal was monitored and the amplitude of the oscillation of the swashplate was increased until either an adequate signal at the forcing frequency was obtained in the blade chordwise bending moment, or until a load limit was reached at any of the instrumented blade stations. Abrupt termination of the excitation yielded the transient decay of the blade edgewise bending moment signal which was recorded and analyzed using the moving block technique. Several stability records were obtained at each operating condition. Details of the transient decay analysis technique are presented below.

PERFORMANCE DATA

Performance data and rotor control positions are presented in table format in appendix A. The data are presented with test points grouped for conditions with the same rotor rotational speed and are ordered in terms of increasing lift coefficient (CLR/S). All testing was done at a shaft angle of -10° with the wind tunnel access doors open. Although all testing was done in this manner, a slight buildup of tunnel air velocity occurred within the test section as a data run progressed. This buildup yielded a dynamic pressure indication in the tunnel's instrumentation and data system which resulted in nonzero VKNOTS for some data points.

AEROELASTIC STABILITY DATA

The primary objective of the test was to investigate the rotor's aeroelastic inplane stability characteristics. Stability data are presented in appendix B as time-to-half amplitude, T 1/2 (sec), real part of measured damping exponent, SIGMA (sec^{-1}), and fixed system damping coefficient, ZETA. The data presented are grouped for conditions with the same rotational speed and are ordered in terms of increasing lift coefficient (CLR/S). (Note that appendix B does include stability data (run 3, 350 rpm) that does not have corresponding performance, rotor loads or rotor test apparatus vibration data elsewhere in the report.) Values for the rotor thrust coefficient (CT/S) and the rotor control positions (A1 and B1) for this particular run are included in appendix B. Repeated run-point numbers imply multiple stability evaluations for the same trim operating condition. The damping coefficient ZETA was calculated using the experimentally determined ω_ζ.

System stability determination was performed using a transient decay time history from an edgewise bending moment signal (station 0.10R). An 8-sec portion of the decaying analog signal was recorded for analysis. Using an appropriately selected 5-sec portion of the time history, the transient signal was analyzed using the moving block technique (ref. 3) at the fundamental edgewise bending frequency. For a typical analysis record, the fundamental mode was around 4.6 Hz. The moving block technique assumes the decaying transient is a lightly damped, single-degree-of-freedom, sinusoidal signal. A discrete Fourier transform of the recorded signal is calculated using only a portion (or block) of the sample record. In this investigation, a block size of one quarter (or 1.25 sec) was used exclusively. The natural logarithm of the magnitude of the Fourier coefficient at the analysis frequency is then plotted versus time; the time is given by the location in the original record where the analyzed block of data begins. Consequently, a 5-sec record length using a 1.25-sec block size yields a 3.75-sec logarithm plot. Fitting a straight line through these data yields a slope proportional to the decay coefficient, SIGMA (sec^{-1}), of the equivalent single-degree-of-freedom system.

Stability data for 350, 375, 400, and 425 rpm are shown in figures 3-6. Each plotted point represents a unique data record. An effort was made to evaluate the repeatability of the stability determinations. (At most test conditions, at least four stability determinations were made.) The repeatability of the damping determinations at low-thrust conditions was found to be very good. At the higher thrust conditions, the repeatability of the damping values was poor. Fortunately, when the system is heavily damped the stability determination is not critical. In general, the scatter in the experimentally determined decay coefficients is small at low values of rotor thrust and increases as rotor thrust increases. The experimental data have been curve-fit with a second-order, least-squares, polynomial regression curve for each rpm.

Stability data for 350 rpm are shown in figure 3. From the least-squares, curve-fit of the experimental data, a minimum damping level is obtained at a C_T/σ value of about 0.012. A C_T/σ value of 0.012 corresponds to a decay coefficient of -0.47 (sec^{-1}).

Stability data for 375 rpm are shown in figure 4. At this rotational speed, a minimum damping level was obtained at a C_T/σ value of about 0.016. The decay coefficient at this C_T/σ value is -0.47 (sec^{-1}). There was little scatter in the

experimentally determined decay coefficients over the entire thrust range tested at this rotational speed.

Stability data for 400 rpm are shown in figure 5. From the curve-fit of the data, a minimum damping level occurs at a C_T/σ value of about 0.019 which corresponds to decay coefficient of -0.46 (sec^{-1}). The minimum in damping for all rpms and thrust settings tested occurred at this condition (400 rpm and a C_T/σ value about 0.019).

Stability data for 425 rpm (design rotational speed) are shown in figure 6. As with the other rotational speeds tested, the experimental data show an increase in damping with increasing rotor thrust. At high thrust values, data scatter is increased. The minimum damping value for 425 rpm was found to be at a C_T/σ value of about 0.024. A C_T/σ value of 0.024 corresponds to a value of SIGMA (decay coefficient) equal to -0.54 (sec^{-1}).

The overall trend is the same for each rotor rotational speed tested. Damping was found to increase as rotor thrust was increased above about $C_T/\sigma = 0.02$ (constant rpm). Damping increased as rotational speed was increased at constant thrust conditions from 350 to 400 rpm. Damping trends with constant rotor thrust and changing rotor speed are summarized in figure 7. The experimental data have been curve-fit with a second-order, least-squares, polynomial regression curve for 350, 375, 400, and 425 rpm as shown in figures 3-6. Constant rotor thrust contours (C_T/σ = 0.0, 0.02, 0.04, 0.06, 0.08) are drawn. At constant rotor thrust, damping reduces to a minimum at 400 rpm. At this operating condition, the measured inplane regressing mode frequency ($\Omega - \omega_\zeta$) was determined to be in resonance with the longitudinal balance mode at 2.24 Hz (fig. 8). Consequently, a ground resonance condition exists at this rotor rotational speed. Yet, due to the large fixed system inertia of the test apparatus and the balance system, the rotor system inplane damping is sufficient to maintain a stable operating condition. As rotor speed is increased from 400 to 425 rpm, the damping increases for all rotor thrust levels. From figure 7, the increase in damping at C_T/σ of 0.0 relative to a C_T/σ of 0.02 is clearly seen for each rotor rotational speed.

ROTOR LOADS DATA

Steady-state dynamic rotor loads data were obtained at each test condition. The measurements and their positive sign conventions are given in table 4. The data are presented in table format in appendix C with test points grouped for conditions with the same rotor rpm and are ordered in terms of increasing lift coefficient (CLR/S). The same run-point sequence as in appendix A is used. For each of the measurements, the time-average mean and root-mean-square values are presented. Data were acquired over a period of approximately 1 sec (eight rotor revolution cycles). The existence of time-dependent rotor loads in a hovering rotor condition may be due to several sources: rotor disk inflow asymmetry, the presence of the fuselage body beneath the rotor disk in the wake, test section rotor wake recirculation, and the presence of some slight air flow through the test section.

ROTOR TEST APPARATUS VIBRATION DATA

The fourth harmonic magnitude and phase angle data from accelerometers mounted on the rotor test apparatus are presented in table format in appendix D for all conditions tested. The accelerometers used are listed in table 5. Their locations on the test apparatus are shown in figure 9. The same run-point sequence as in appendix A is used.

CONCLUDING REMARKS

A full-scale hingeless rotor system was tested in hover in the NASA Ames 40- by 80-Foot Wind Tunnel. Rotor aeroelastic stability, performance, and loads data were investigated. Rotor rotational speed and thrust were varied. Rotor inplane performance, blade loads and vibration levels in the test apparatus are presented for all operating conditions tested. Aeroelastic stability characteristics of the rotor blade's fundamental inplane bending mode were investigated in hover using the moving-block technique. The rotor was stable at all conditions tested. At constant rotor rotational speed, a minimum inplane damping level was obtained as thrust was reduced (at approximately $C_T/\sigma = 0.02$). At constant rotor lift, a minimum in rotor inplane damping was measured at 400 rpm.

APPENDIX A

The following tables present hover performance and control positions data for the BO-105 rotor system. The run/point number sequence used is based on rotor rpm and rotor lift coefficient (CLR/S). The run/point numbers are ordered in terms of increasing rotor lift coefficient at each rotor rpm tested.

NOMENCLATURE

A1,B1	coefficients in the representation of rotor blade cyclic pitch, $-A1\cos(\psi + 10°) - B1\sin(\psi + 10°)$, deg
CLR/S	rotor lift coefficient, positive vertical, rotor lift/$\rho S(\Omega R)^2$
CMX/S	rotor rolling moment coefficient, positive advancing side of rotor disk down, rotor rolling moment/$\rho S(\Omega R)^2 R$
CMY/S	rotor pitching moment coefficient, positive leading side of rotor disk up, rotor pitching moment/$\rho S(\Omega R)^2 R$
CMZ/S	rotor yawing moment coefficient, positive opposing direction of rotation, rotor yawing moment/$\rho S(\Omega R)^2 R$
CP/S	rotor power coefficient, rotor power/$\rho S(\Omega R)^3$
CPO/S	non-ideal rotor power coefficient, CPO/S = CP/S - CQ/S + CQO/S
CQ/S	rotor torque coefficient, rotor torque/$\rho\pi R^3(\Omega R)^2$
CQO/S	non-ideal rotor torque coefficient, CQO/S = $(1/\sqrt{2})(CLR/S)^{3/2}(S/\pi R^2)^{1/2}$
CXR/S	rotor propulsive force coefficient, positive toward leading side of rotor disk, -drag/$\rho S(\Omega R)^2$
CYR/S	rotor side force coefficient, positive toward advancing side of rotor disk, rotor side force/$\rho S(\Omega R)^2$
OMEGA*R,ΩR	rotor blade tip speed, m/sec
RHO	air density, kg/m^3
rpm	rotor rotational speed, rev/min
THETA,θ	collective pitch setting at 0.7R, deg
TIPM	rotor rotational Mach number, $\Omega R/c$
VKNOTS,V	free stream velocity, knots

RUN.PT	TIPM RHO	OMEG*R RPM	THETA VKNOTS	A1 B1	CLP/S CMY/S	CXR/S CMZ/S	CYR/S CMX/S	CP/S CPO/S
5.15	0.5253	180.0	0.8	-0.4	-0.004081	-0.000423	0.000043	0.001372
	1.2064	350.0	0.0	-0.1	-0.000586	0.001401	-0.000892	-0.010397
5.14	0.5253	180.0	1.8	-0.2	-0.001095	-0.000107	-0.000021	0.000978
	1.2064	350.0	0.0	-0.2	-0.000207	0.001331	-0.000631	0.000130
5.13	0.5283	181.0	2.9	-0.2	0.002441	0.000594	-0.000191	0.000929
	1.2067	352.0	0.0	-0.4	-0.000177	0.001455	-0.000217	0.000905
5.16	0.5251	180.0	3.8	0.0	0.005996	0.001246	0.000129	0.001102
	1.2057	350.0	0.0	-0.2	-0.000293	0.001404	-0.000294	0.001012
5.12	0.5253	180.0	5.5	0.0	0.019864	0.003608	0.000107	0.001550
	1.2066	350.0	4.2	0.0	-0.000689	0.002113	-0.000160	0.001013
5.11	0.5268	180.5	6.3	-0.1	0.024982	0.004270	-0.000363	0.001927
	1.2056	351.0	0.0	-0.2	-0.000174	0.002393	-0.000458	0.001172
5.17	0.5251	180.0	9.9	-0.3	0.043480	0.007430	-0.000236	0.003103
	1.2056	350.0	0.0	-0.6	0.000589	0.003388	-0.000627	0.001369
5.18	0.5251	180.0	8.9	-1.1	0.044083	0.009994	-0.000860	0.003144
	1.2056	350.0	4.2	2.0	-0.005500	0.003605	-0.000851	0.001349

RUN.PT	TIPM RHO	OMEG*R RPM	THETA VKNOTS	A1 B1	CLF/S CMY/S	CXR/S CMZ/S	CYR/S CMX/S	CP/S CPO/S
5.19	0.5251	130.0	9.0	0.2	0.045029	0.006255	0.000473	0.003065
	1.2056	350.0	4.6	-2.2	0.003586	0.003564	-0.000673	0.001254
5.20	0.5251	180.0	9.0	-1.4	0.045265	0.010102	-0.000989	0.003179
	1.2056	350.0	3.0	1.9	-0.005356	0.003564	-0.001290	0.001313
5.10	0.5253	180.0	8.5	-0.1	0.043810	0.007516	-0.000322	0.003066
	1.2066	350.0	0.0	-0.2	-0.000039	0.003769	-0.000656	0.001313
5. 6	0.5254	180.0	8.9	-0.1	0.049029	0.008136	-0.000515	0.003432
	1.2071	350.0	4.9	-0.2	-0.000173	0.003917	-0.001308	0.001359
5. 9	0.5268	180.5	10.6	-0.1	0.063792	0.010721	-0.001132	0.004799
	1.2064	351.0	5.5	-0.2	0.000444	0.005566	-0.000650	0.001721
5. 8	0.5253	180.0	10.9	-0.1	0.068148	0.011555	0.000043	0.005076
	1.2065	350.0	0.0	-0.1	-0.000007	0.005183	-0.001144	0.001677
5. 7	0.5253	180.0	13.0	-0.1	0.089894	0.015444	-0.000021	0.007499
	1.2063	350.0	4.2	-0.1	-0.001431	0.008099	-0.001071	0.002345
7. 5	0.5605	192.8	1.8	-0.2	-0.001642	-0.000151	0.000151	0.001025
	1.1959	375.0	0.0	-0.2	0.000088	0.000924	-0.000284	-0.001008

RUN.PT	TIPM RHO	OMEG*R RPM	THETA VKNOTS	A1 B1	CLR/S CMY/S	CXR/S CMZ/S	CYR/S CMX/S	CP/S CPO/S
7. 5	0.5605	192.3	0.8	-0.3	-0.005493	-0.000849	0.000208	0.001167
	1.1958	375.0	0.0	-0.1	-0.000128	0.001100	-0.000453	-0.021578
7. 4	0.5590	192.3	2.9	-0.3	0.001860	0.000513	0.000323	0.000949
	1.1955	374.0	3.9	-0.5	-0.000206	0.000852	-0.000400	0.000932
7. 3	0.5604	192.3	4.9	-0.1	0.013548	0.002510	0.000453	0.001356
	1.1962	375.0	3.0	-0.1	-0.000009	0.001081	-0.001120	0.001053
6. 6	0.5574	192.3	7.1	-0.5	0.028402	0.004928	-0.000477	0.002160
	1.1881	374.0	0.0	-0.6	0.000571	0.001985	-0.000960	0.001244
6. 5	0.5605	193.3	3.8	-0.5	0.044043	0.007136	0.000076	0.003187
	1.1893	376.0	0.0	-0.4	0.000914	0.002764	-0.001294	0.001424
6. 3	0.5589	192.8	8.8	-0.2	0.045792	0.007832	-0.000608	0.003388
	1.1884	375.0	3.5	0.0	0.000170	0.003398	-0.001131	0.001514
6. 4	0.5574	192.3	10.7	-0.3	0.068914	0.011400	-0.000707	0.005318
	1.1894	374.0	4.6	0.2	0.000178	0.005022	-0.001782	0.001865
8. 7	0.5985	205.7	2.6	-0.3	0.000083	-0.000017	-0.000215	0.001004
	1.2021	400.0	0.0	-0.5	0.000119	0.001660	0.000141	0.001004

RUN.PT	TIPM RHO	OMEG*R RPM	THETA VKNOTS	A1 B1	CLP/S CMY/S	CXR/S CMZ/S	CYR/S CMX/S	CP/S CPO/S
8. 6	0.6001	206.2	6.3	-0.3	0.021086	0.003512	-0.000377	0.001693
	1.2030	401.0	0.0	-0.5	-0.000183	0.002280	-0.000180	0.001108
8. 5	0.5989	205.7	8.7	-0.4	0.040434	0.006758	-0.000429	0.002861
	1.2035	400.0	0.0	-0.5	-0.000199	0.003703	-0.000821	0.001309
7. 7	0.5980	205.7	8.9	-0.4	0.042292	0.007413	0.000282	0.002921
	1.1962	400.0	0.0	-0.5	-0.000541	0.002766	-0.000885	0.001257
8. 4	0.5992	205.7	10.4	-0.1	0.061098	0.010392	-0.000642	0.004342
	1.2046	400.0	0.0	-0.1	-0.001544	0.005026	-0.000695	0.001456
7. 9	0.5993	206.2	11.7	-0.3	0.067515	0.012251	0.000479	0.005171
	1.1955	401.0	7.8	-0.7	-0.000777	0.005232	-0.001584	0.001808
7. 8	0.5980	205.7	12.4	-0.4	0.075563	0.012887	0.001144	0.005938
	1.1962	400.0	5.2	-0.6	-0.000207	0.005622	-0.002412	0.001968
10. 7	0.6336	218.5	3.3	-0.2	-0.000044	0.000514	0.000265	0.001087
	1.1956	425.0	3.9	-0.4	-0.001039	0.000994	-0.000322	0.001082
10. 6	0.6336	218.5	6.7	-0.3	0.019913	0.003894	-0.000162	0.001842
	1.1958	425.0	4.3	-0.5	-0.000707	0.001607	-0.000583	0.001302

RUN.PT	TIPM RHO	OMEG*R RPM	THETA VKNOTS	A1 B1	CLP/S CMY/S	CXR/S CMZ/S	CYR/S CMX/S	CP/S CPO/S
8. 9	0.6359	218.5	8.9	-0.4	0.038918	0.006579	-0.000614	0.002866
	1.2025	425.0	3.9	-0.4	-0.001228	0.003621	-0.000595	0.001398
10. 5	0.6322	218.0	8.9	-0.4	0.039657	0.006348	-0.000369	0.002991
	1.1963	424.0	0.0	-0.3	-0.000028	0.002735	-0.000848	0.001481
8. 8	0.6359	218.5	8.9	-0.4	0.041104	0.007211	-0.001004	0.003093
	1.1552	425.0	0.0	-0.4	-0.001171	0.003677	-0.000229	0.001498
9. 7	0.6340	218.5	11.2	-0.5	0.061961	0.010604	-0.000074	0.004791
	1.1949	425.0	6.3	-0.8	0.000298	0.004763	-0.001679	0.001843
9. 6	0.6341	218.5	11.8	-0.5	0.068577	0.011804	-0.001058	0.005423
	1.1954	425.0	3.9	-0.7	-0.001148	0.006476	-0.000305	0.001989
9. 5	0.6343	218.5	13.0	-0.2	0.078788	0.012678	0.000015	0.006412
	1.1962	425.0	0.0	-1.0	0.000762	0.007116	-0.001036	0.002195
9. 4	0.6344	218.5	14.9	-0.3	0.104688	0.017392	-0.000073	0.009573
	1.1964	425.0	11.0	-1.0	-0.001426	0.011102	-0.001962	0.003106
9. 3	0.6345	218.5	16.5	-0.2	0.119362	0.019211	-0.000543	0.012141
	1.1965	425.0	6.7	-1.1	0.000259	0.013135	0.000048	0.004278

APPENDIX B

The following tables present BO-105 rotor stability data. The stability data are presented as time-to-half amplitude, T 1/2 (sec), real part of measured damping exponent, SIGMA (sec^{-1}), and fixed system damping coefficient, ZETA. The damping coefficient was calculated using the experimentally determined ω_ζ.

Data are presented in the same run/point number sequence as appendix A. At some run/point numbers, only performance data were obtained. At others, one or more stability determinations were made.

NOMENCLATURE

A1,B1	coefficients in the representation of rotor blade cyclic pitch, $-A1 \cos(\psi + 10°) - B1 \sin(\psi + 10°)$, deg
CT/S	rotor thrust coefficient, positive vertical, thrust
rpm	rotor rotational speed, rev/min
SIGMA	damping decay coefficient, sec^{-1}
T 1/2	time to half amplitude, sec
ZETA,ζ	fixed system percent critical damping coefficient
ω_ζ	fundamental rotating inplane bending frequency, Hz

RUN.PT	RPM	CT/S	A1	B1	T 1/2	SIGMA	ZETA	ω_ζ
5.15	350.	-0.004	-0.4	-0.1	1.16	-0.60	0.065	4.40
5.15	350.	-0.004	-0.4	-0.1	1.25	-0.56	0.062	4.40
5.15	350.	-0.004	-0.4	-0.1	1.25	-0.55	0.061	4.40
5.15	350.	-0.004	-0.4	-0.1	1.39	-0.50	0.056	4.40
5.15	350.	-0.004	-0.4	-0.1	1.18	-0.59	0.065	4.40
5.14	350.	-0.001	-0.2	-0.2	1.27	-0.55	0.061	4.40
5.14	350.	-0.001	-0.2	-0.2	1.30	-0.53	0.059	4.40
5.13	352.	0.002	-0.2	-0.4	1.47	-0.47	0.052	4.40
5.13	352.	0.002	-0.2	-0.4	1.50	-0.46	0.051	4.40
5.13	352.	0.002	-0.2	-0.4	1.39	-0.50	0.055	4.40
5.13	352.	0.002	-0.2	-0.4	1.39	-0.50	0.056	4.40
5.13	352.	0.002	-0.2	-0.4	1.43	-0.49	0.054	4.40

RUN.PT	RPM	CT/S	A1	B1	T 1/2	SIGMA	ZETA	ω_ζ
5.16	350.	0.006	0.0	-0.2	1.47	-0.47	0.052	4.40
5.16	350.	0.006	0.0	-0.2	1.46	-0.47	0.053	4.40
5.12	350.	0.020	0.0	0.0	1.50	-0.46	0.051	4.40
3. 9	350.	0.021	-0.4	-0.6	1.48	-0.47	0.052	4.40
3. 9	350.	0.021	-0.4	-0.6	1.47	-0.47	0.052	4.40
3. 9	350.	0.021	-0.4	-0.6	1.38	-0.50	0.056	4.40
3. 9	350.	0.021	-0.4	-0.6	1.40	-0.49	0.055	4.40
3. 8	350.	0.039	-0.4	-0.6	1.09	-0.64	0.064	4.25
3. 8	350.	0.039	-0.4	-0.6	1.10	-0.63	0.070	4.40
3. 8	350.	0.039	-0.4	-0.6	1.12	-0.62	0.073	4.48
3. 8	350.	0.039	-0.4	-0.6	1.17	-0.59	0.066	4.40
3. 8	350.	0.039	-0.4	-0.6	1.21	-0.57	0.064	4.40

RUN.PT	RPM	CT/S	A1	B1	T 1/2	SIGMA	ZETA	ω_ζ
3. 7	350.	0.062	-0.4	-0.6	0.52	-1.32	0.133	4.25
3. 7	350.	0.062	-0.4	-0.5	0.49	-1.40	0.141	4.25
3. 7	350.	0.062	-0.4	-0.6	0.61	-1.13	0.114	4.25
3. 7	350.	0.062	-0.4	-0.6	0.68	-1.01	0.102	4.25
3. 7	350.	0.062	-0.4	-0.6	0.54	-1.29	0.130	4.25
3. 6	350.	0.079	-0.4	-0.5	0.42	-1.65	0.165	4.25
3. 6	350.	0.079	-0.4	-0.5	0.48	-1.45	0.146	4.25
3. 6	350.	0.079	-0.4	-0.5	0.48	-1.43	0.144	4.25
3. 6	350.	0.079	-0.4	-0.5	0.48	-1.45	0.145	4.25
3. 6	350.	0.079	-0.4	-0.5	0.31	-2.22	0.223	4.25
7. 6	375.	-0.005	-0.3	-0.1	1.22	-0.57	0.055	4.50
7. 6	375.	-0.005	-0.3	-0.1	1.30	-0.53	0.051	4.50

RUN.PT	RPM	CT/S	A1	B1	T 1/2	SIGMA	ZETA	ω_ζ
7. 6	375.	-0.005	-0.3	-0.1	1.20	-0.58	0.056	4.60
7. 6	375.	-0.005	-0.3	-0.1	1.15	-0.60	0.058	4.60
7. 5	375.	-0.002	-0.2	-0.2	1.26	-0.55	0.053	4.60
7. 5	375.	-0.002	-0.2	-0.2	1.28	-0.54	0.052	4.60
7. 4	374.	0.002	-0.3	-0.5	1.37	-0.51	0.049	4.60
7. 4	374.	0.002	-0.3	-0.5	1.44	-0.48	0.047	4.60
7. 4	374.	0.002	-0.3	-0.5	1.35	-0.51	0.049	4.60
7. 4	374.	0.002	-0.3	-0.5	1.34	-0.52	0.050	4.60
7. 3	375.	0.014	-0.1	-0.1	1.45	-0.48	0.046	4.60
7. 3	375.	0.014	-0.1	-0.1	1.48	-0.47	0.045	4.60
7. 3	375.	0.014	-0.1	-0.1	1.48	-0.47	0.045	4.60
7. 3	375.	0.014	-0.1	-0.1	1.49	-0.46	0.045	4.60

RUN.PT	RPM	CT/S	A1	B1	T 1/2	SIGMA	ZETA	ω_ζ
6. 6	374.	0.028	-0.5	-0.6	1.34	-0.52	0.045	4.40
6. 6	374.	0.028	-0.5	-0.6	1.42	-0.49	0.042	4.40
6. 6	374.	0.028	-0.5	-0.6	1.29	-0.54	0.046	4.40
6. 6	374.	0.028	-0.5	-0.6	1.29	-0.54	0.052	4.50
6. 5	376.	0.044	-0.5	-0.4	1.18	-0.59	0.051	4.40
6. 5	376.	0.044	-0.5	-0.4	1.30	-0.53	0.046	4.40
6. 5	376.	0.044	-0.5	-0.4	1.17	-0.59	0.051	4.40
6. 5	375.	0.044	-0.5	-0.4	0.85	-0.81	0.070	4.40
6. 5	376.	0.044	-0.5	-0.4	1.25	-0.56	0.048	4.40
6. 4	374.	0.069	-0.3	0.2	0.67	-1.04	0.089	4.40
6. 4	374.	0.069	-0.3	0.2	0.69	-1.01	0.086	4.40
6. 4	374.	0.069	-0.3	0.2	0.72	-0.97	0.083	4.40

RUN.PT	RPM	CT/S	A1	B1	T 1/2	SIGMA	ZETA	ω_ζ
6. 4	374.	0.069	-0.3	0.2	0.60	-1.16	0.099	4.40
8. 7	400.	0.000	-0.3	-0.5	1.47	-0.47	0.040	4.80
8. 7	400.	0.000	-0.3	-0.5	1.33	-0.52	0.044	4.80
8. 7	400.	0.000	-0.3	-0.5	1.35	-0.51	0.044	4.80
8. 7	400.	0.000	-0.3	-0.5	1.29	-0.54	0.046	4.80
8. 6	401.	0.021	-0.3	-0.5	1.49	-0.46	0.036	4.60
8. 6	401.	0.021	-0.3	-0.5	1.48	-0.47	0.036	4.60
8. 6	401.	0.021	-0.3	-0.5	1.52	-0.46	0.035	4.60
8. 6	401.	0.021	-0.3	-0.5	1.44	-0.48	0.037	4.60
8. 5	400.	0.040	-0.4	-0.5	1.32	-0.53	0.040	4.60
8. 5	400.	0.040	-0.4	-0.5	1.28	-0.54	0.042	4.60
8. 5	400.	0.040	-0.4	-0.5	1.14	-0.61	0.047	4.60

RUN.PT	RPM	CT/S	A1	B1	T 1/2	SIGMA	ZETA	ω_ζ
3. 5	400.	0.040	-0.4	-0.5	1.24	-0.56	0.043	4.60
7. 7	400.	0.042	-0.4	-0.5	1.29	-0.54	0.041	4.60
7. 7	400.	0.042	-0.4	-0.5	1.21	-0.57	0.044	4.60
6. 4	400.	0.061	-0.1	-0.1	0.97	-0.71	0.055	4.60
6. 4	400.	0.061	-0.1	-0.1	1.19	-0.58	0.045	4.60
6. 4	400.	0.061	-0.1	-0.1	1.10	-0.63	0.048	4.60
6. 4	400.	0.061	-0.1	-0.1	1.03	-0.67	0.052	4.60
7. 9	401.	0.068	-0.3	-0.7	0.68	-1.02	0.072	4.40
7. 9	401.	0.068	-0.3	-0.7	0.79	-0.88	0.062	4.40
7. 9	401.	0.068	-0.3	-0.7	0.78	-0.89	0.062	4.40
7. 9	401.	0.068	-0.3	-0.7	0.74	-0.93	0.065	4.40
7. 8	400.	0.076	-0.4	-0.6	0.81	-0.85	0.060	4.40

RUN.PT	RPM	CT/S	A1	B1	T 1/2	SIGMA	ZETA	ω_ζ
7. 8	400.	0.076	-0.4	-0.6	0.84	-0.83	0.058	4.40
7. 8	400.	0.076	-0.4	-0.6	0.56	-1.25	0.088	4.40
7. 8	400.	0.076	-0.4	-0.6	0.73	-0.95	0.067	4.40
10. 7	425.	0.000	-0.2	-0.4	1.17	-0.59	0.041	4.80
10. 7	425.	0.000	-0.2	-0.4	1.16	-0.60	0.042	4.80
10. 7	425.	0.000	-0.2	-0.4	1.17	-0.59	0.041	4.80
10. 7	425.	0.000	-0.2	-0.4	1.20	-0.58	0.040	4.80
10. 6	425.	0.020	-0.3	-0.5	1.24	-0.56	0.039	4.80
10. 6	425.	0.020	-0.3	-0.5	1.26	-0.55	0.038	4.80
10. 6	425.	0.020	-0.3	-0.5	1.17	-0.59	0.041	4.80
10. 6	425.	0.020	-0.3	-0.5	1.12	-0.62	0.043	4.80
10. 5	424.	0.040	-0.4	-0.3	1.00	-0.69	0.044	4.60

RUN.PT	RPM	CT/S	A1	B1	T 1/2	SIGMA	ZETA	ω_ζ
10. 5	424.	0.040	-0.4	-0.3	1.04	-0.67	0.043	4.60
10. 5	424.	0.040	-0.4	-0.3	1.16	-0.60	0.038	4.60
8. 8	425.	0.041	-0.4	-0.4	1.01	-0.69	0.044	4.80
8. 8	425.	0.041	-0.4	-0.4	1.01	-0.68	0.048	4.60
8. 9	425.	0.041	-0.4	-0.4	1.07	-0.65	0.041	4.60
8. 8	425.	0.041	-0.4	-0.4	1.06	-0.65	0.042	4.60
9. 7	425.	0.062	-0.5	-0.8	0.91	-0.73	0.049	4.60
9. 7	425.	0.062	-0.5	-0.8	1.06	-0.65	0.042	4.60
9. 7	425.	0.062	-0.5	-0.8	0.77	-0.90	0.058	4.60
9. 7	425.	0.062	-0.5	-0.8	0.88	-0.79	0.051	4.60
9. 6	425.	0.069	-0.5	-0.7	0.80	-0.87	0.056	4.60
9. 6	425.	0.069	-0.5	-0.7	0.81	-0.86	0.055	4.60

RUN.PT	RPM	CT/S	A1	B1	T 1/2	SIGMA	ZETA	ω_ζ
9. 6	425.	0.069	-0.5	-0.7	0.82	-0.84	0.054	4.60
9. 6	425.	0.069	-0.5	-0.7	0.94	-0.74	0.047	4.60
9. 5	425.	0.079	-0.2	-1.0	0.50	-1.38	0.089	4.60
9. 5	425.	0.079	-0.2	-1.0	0.55	-1.27	0.081	4.60
9. 5	425.	0.079	-0.2	-1.0	0.71	-0.98	0.063	4.60
9. 5	425.	0.079	-0.2	-1.0	0.56	-1.24	0.079	4.60
9. 4	425.	0.105	-0.3	-1.0	0.31	-2.21	0.141	4.60
9. 4	425.	0.105	-0.3	-1.0	0.38	-1.84	0.118	4.60
9. 4	425.	0.105	-0.3	-1.0	0.47	-1.47	0.094	4.60
9. 4	425.	0.105	-0.3	-1.0	0.55	-1.25	0.080	4.60
9. 3	425.	0.119	-0.2	-1.1	0.25	-2.74	0.163	4.40

APPENDIX C

The following tables present BO-105 rotor loads data. The data are presented in the same run/point number sequence as appendices A and B. The channel designations are as follows:

Blade number	Measurement	Channel designation	Positive sign convention
1	Chord bend STA = 0.10R	A	Leading edge in tension
3	Chord bend STA = 0.10R	B	Leading edge in tension
1	Flap bend STA = 0.10R	C	Flapping up
1	Flap bend STA = 0.28R	D	Flapping up
1	Chord bend STA = 0.57R	E	Leading edge in tension
1	Flap bend STA = 0.57R	F	Flapping up
1	Flap bend STA = 0.80R	G	Flapping up
1	Torsion STA = 0.34R	H	Leading edge up
1	Pitch link	I	Tension

RUN.PT		CHANNEL DESIGNATION							
		A	B	C	D	E	F	G	H	I
5.15										
	MEAN	-192585.	-111338.	-166242.	-7912.	-32736.	-4251.	-2740.	-2004.	705.
	RMS	736.	346.	445.	32.	417.	46.	62.	5.	5.
5.14										
	MEAN	-191090.	-107499.	-165156.	-7095.	-32959.	-2684.	-714.	-2018.	731.
	RMS	710.	257.	551.	27.	436.	26.	51.	5.	10.
5.13										
	MEAN	-175914.	-102142.	-152587.	-6963.	-34009.	-2328.	-313.	-2654.	897.
	RMS	669.	224.	430.	21.	297.	26.	51.	5.	9.
5.16										
	MEAN	-182428.	-94420.	-160257.	-6375.	-33326.	-2845.	-108.	-2583.	1003.
	RMS	823.	337.	698.	28.	277.	36.	41.	8.	13.
5.12										
	MEAN	-120177.	-73521.	-122997.	-4911.	-33018.	-2441.	-47.	-3287.	1050.
	RMS	562.	297.	371.	31.	325.	64.	76.	8.	6.
5.11										
	MEAN	-115043.	-57020.	-119809.	-4283.	-32822.	-2222.	-135.	-3570.	1112.
	RMS	569.	468.	579.	46.	584.	69.	86.	10.	9.
5.17										
	MEAN	-137078.	-43897.	-123312.	-1666.	-29865.	-518.	841.	-3943.	1259.
	RMS	676.	593.	805.	69.	690.	174.	212.	17.	5.
5.18										
	MEAN	-129674.	-49265.	-115366.	-1938.	-30632.	-701.	650.	-4153.	1513.
	RMS	4834.	2323.	5157.	213.	1102.	216.	188.	36.	45.
5.19										
	MEAN	-128150.	-48377.	-114239.	-2025.	-31624.	-836.	509.	-4396.	1625.
	RMS	5249.	2462.	5631.	228.	1063.	147.	154.	34.	48.

RUN.PT		CHANNEL DESIGNATION							
		A	B	C	D	E	F	G	H	I
5.20										
	MEAN	-131083.	-49976.	-114996.	-2036.	-30697.	-812.	811.	-4265.	1738.
	RMS	7279.	2530.	7904.	348.	1277.	179.	258.	45.	55.
5.10										
	MEAN	-93943.	-44538.	-104018.	-2024.	-30295.	-602.	523.	-3978.	1203.
	RMS	952.	522.	960.	47.	314.	178.	215.	19.	11.
5. 6										
	MEAN	-91330.	-37273.	-101680.	-1147.	-30060.	-240.	1177.	-4020.	1240.
	RMS	735.	499.	794.	46.	285.	143.	189.	15.	9.
5. 9										
	MEAN	-70541.	-21235.	-79907.	565.	-28799.	1034.	1595.	-4325.	1232.
	RMS	1203.	511.	1151.	45.	421.	171.	243.	18.	9.
5. 8										
	MEAN	-61596.	-15466.	-72233.	1249.	-28629.	1526.	1547.	-4526.	1219.
	RMS	1052.	572.	1255.	60.	572.	186.	251.	15.	6.
5. 7										
	MEAN	-20009.	11868.	-27780.	4413.	-26045.	3237.	1610.	-5004.	1115.
	RMS	876.	629.	1050.	72.	602.	244.	344.	22.	6.
7. 5										
	MEAN	-209944.	-108485.	-180916.	-6748.	-40091.	-3511.	-1356.	-3433.	1167.
	RMS	489.	193.	404.	20.	216.	20.	54.	8.	4.
7. 5										
	MEAN	-209887.	-115324.	-183255.	-7409.	-38609.	-4858.	-3568.	-3169.	975.
	RMS	582.	200.	467.	39.	387.	32.	107.	6.	5.
7. 4										
	MEAN	-195304.	-103499.	-177753.	-6437.	-41573.	-2791.	-818.	-3760.	1258.
	RMS	666.	182.	551.	22.	226.	17.	59.	5.	11.

RUN.PT		CHANNEL DESIGNATION							
		A	B	C	D	E	F	G	H	I
7. 3	MEAN	-134560.	-82713.	-136666.	-5485.	-41490.	-3092.	-782.	-4717.	1434.
	RMS	84.	545.	279.	42.	147.	52.	65.	8.	2.
6. 6	MEAN	-130903.	-56395.	-135571.	-3973.	-37261.	-2225.	203.	-4540.	1492.
	RMS	527.	597.	692.	64.	314.	82.	115.	13.	10.
6. 5	MEAN	-97964.	-42605.	-104324.	-1927.	-35463.	-892.	831.	-5075.	1544.
	RMS	874.	592.	992.	64.	480.	121.	204.	18.	11.
6. 3	MEAN	-80979.	-36345.	-107629.	-1439.	-34442.	-529.	437.	-5100.	1372.
	RMS	525.	285.	423.	67.	507.	127.	142.	14.	8.
6. 4	MEAN	-55599.	-12929.	-86159.	720.	-31952.	561.	1002.	-5541.	1459.
	RMS	533.	497.	760.	102.	693.	182.	299.	27.	5.
8. 7	MEAN	-203181.	-109631.	-182025.	-4947.	-46646.	-2940.	-1164.	-4783.	1177.
	RMS	570.	202.	442.	35.	250.	29.	91.	7.	11.
8. 6	MEAN	-169843.	-82087.	-149925.	-3349.	-43268.	-3072.	-459.	-5798.	1728.
	RMS	898.	492.	926.	57.	278.	86.	138.	14.	13.
8. 5	MEAN	-128160.	-50140.	-125965.	-1260.	-43302.	-1641.	461.	-7092.	1904.
	RMS	609.	456.	754.	38.	415.	114.	183.	18.	9.
7. 7	MEAN	-161184.	-46993.	-158136.	-1867.	-41735.	-1214.	125.	-7006.	2205.
	RMS	346.	430.	460.	70.	662.	158.	209.	26.	5.

RUN.PT		CHANNEL DESIGNATION							
		A	B	C	D	E	F	G	H	I
8. 4										
	MEAN	-80288.	-19951.	-102561.	1269.	-39943.	143.	938.	-7433.	1837.
	RMS	869.	436.	1016.	86.	3052.	185.	232.	53.	10.
7. 9										
	MEAN	-74136.	-11263.	-84557.	660.	-39074.	-47.	830.	-7626.	2007.
	RMS	1059.	619.	1144.	100.	1836.	231.	310.	44.	10.
7. 8										
	MEAN	-80285.	-198.	-71715.	1758.	-37074.	1343.	1088.	-7833.	1922.
	RMS	851.	556.	785.	105.	1207.	251.	362.	37.	7.
10. 7										
	MEAN	-217246.	-107571.	-202089.	-4341.	-46276.	-2950.	-562.	-5293.	1823.
	RMS	434.	353.	364.	40.	191.	41.	91.	9.	10.
10. 6										
	MEAN	-180455.	-74068.	-170040.	-3031.	-45020.	-3161.	-173.	-7196.	2292.
	RMS	261.	227.	155.	40.	205.	72.	120.	15.	6.
8. 9										
	MEAN	-154881.	-50894.	-149046.	-819.	-46181.	-1699.	358.	-8193.	2287.
	RMS	357.	551.	548.	61.	343.	161.	181.	35.	6.
10. 5										
	MEAN	-135457.	-46318.	-155854.	-1034.	-42793.	-1404.	529.	-7339.	2137.
	RMS	650.	474.	583.	71.	464.	160.	273.	32.	6.
8. 8										
	MEAN	-170629.	-51824.	-170748.	-743.	-42557.	-1773.	-67.	-7733.	2233.
	RMS	323.	309.	430.	72.	703.	119.	181.	23.	5.
9. 7										
	MEAN	-83087.	-17750.	-96287.	269.	-41604.	94.	966.	-8334.	1867.
	RMS	765.	516.	1082.	79.	825.	135.	261.	32.	4.

RUN.PT		CHANNEL DESIGNATION							
		A	B	C	D	E	F	G	H	I
9. 6										
	MEAN	-58627.	-8065.	-77661.	996.	-40921.	783.	815.	-8480.	1789.
	RMS	697.	525.	845.	94.	732.	186.	301.	42.	9.
9. 5										
	MEAN	-16196.	8570.	-61911.	2140.	-40175.	905.	946.	-8880.	1728.
	RMS	933.	614.	1093.	112.	1125.	238.	366.	53.	7.
9. 4										
	MEAN	54514.	40838.	5478.	4187.	-34891.	2978.	448.	-8879.	1295.
	RMS	1128.	754.	1472.	107.	1255.	289.	376.	83.	14.
9. 3										
	MEAN	133951.	83588.	74789.	7311.	-29358.	5787.	-41.	-8250.	636.
	RMS	1848.	806.	1977.	93.	818.	188.	400.	57.	9.

APPENDIX D

The fourth harmonic magnitude and phase angle data from accelerometers mounted on the rotor test apparatus are presented in the following tables. The accelerometer locations on the test apparatus are shown in figure 9. The data are presented in the same run/point sequence as in appendices A, B, and C. The channel designations are as follows:

Location on RTA	Channel designation	Direction
Nose	1	Vertical
Transmission	2	Longitudinal
Tail	3	Longitudinal
Right side	4	Longitudinal
Tail	5	Lateral
Left side	6	Lateral
Right side	7	Lateral

RUN.PT	CHANNEL DESIGNATION						
	1	2	3	4	5	6	7
5.15							
4P MAG	0.87E-02	0.11E-01	0.26E-02	0.41E-02	0.21E-01	0.91E-02	0.89E-02
PHASE	90.	-118.	-73.	110.	116.	-72.	103.
5.14							
4P MAG	0.46E-02	0.86E-02	0.17E-02	0.37E-02	0.38E-01	0.15E-01	0.15E-01
PHASE	168.	-46.	-25.	-179.	-168.	2.	180.
5.13							
4P MAG	0.40E-02	0.72E-02	0.32E-02	0.24E-02	0.49E-01	0.21E-01	0.21E-01
PHASE	152.	-43.	-27.	-166.	-94.	74.	-105.
5.16							
4P MAG	0.99E-03	0.52E-02	0.92E-03	0.16E-02	0.16E-01	0.73E-02	0.71E-02
PHASE	-163.	51.	113.	-61.	-27.	141.	-43.
5.12							
4P MAG	0.50E-02	0.16E-01	0.74E-02	0.82E-02	0.18E-01	0.63E-02	0.65E-02
PHASE	-93.	92.	127.	-55.	121.	-72.	116.
5.11							
4P MAG	0.20E-01	0.28E-01	0.14E-01	0.21E-01	0.85E-01	0.34E-01	0.32E-01
PHASE	55.	-153.	-129.	52.	38.	-148.	27.
5.17							
4P MAG	0.13E-01	0.18E-01	0.54E-02	0.45E-02	0.93E-01	0.41E-01	0.39E-01
PHASE	-52.	121.	-152.	63.	118.	-78.	104.
5.18							
4P MAG	0.12E-01	0.30E-01	0.97E-02	0.15E-01	0.13E+00	0.57E-01	0.54E-01
PHASE	20.	-178.	-112.	84.	102.	-90.	87.
5.19							
4P MAG	0.97E-02	0.19E-01	0.53E-02	0.71E-02	0.47E-01	0.22E-01	0.20E-01
PHASE	21.	157.	-151.	40.	86.	-102.	75.

RUN.PT	CHANNEL DESIGNATION						
	1	2	3	4	5	6	7
5.20							
4P MAG	0.25E-01	0.24E-01	0.37E-02	0.72E-02	0.79E-01	0.30E-01	0.30E-01
PHASE	-141.	21.	42.	-104.	-95.	75.	-107.
5.10							
4P MAG	0.17E-01	0.25E-01	0.18E-01	0.21E-01	0.10E+00	0.39E-01	0.36E-01
PHASE	155.	-44.	-25.	175.	-144.	20.	-158.
5. 6							
4P MAG	0.67E-02	0.79E-02	0.15E-02	0.28E-02	0.53E-01	0.21E-01	0.21E-01
PHASE	126.	-124.	-144.	108.	128.	-63.	114.
5. 9							
4P MAG	0.14E-01	0.26E-01	0.97E-02	0.14E-01	0.32E-01	0.13E-01	0.14E-01
PHASE	28.	-168.	-138.	31.	-10.	-179.	-7.
5. 8							
4P MAG	0.78E-02	0.92E-02	0.74E-02	0.14E-01	0.11E+00	0.40E-01	0.39E-01
PHASE	107.	-99.	-64.	114.	75.	-114.	62.
5. 7							
4P MAG	0.15E-01	0.18E-01	0.13E-01	0.13E-01	0.90E-01	0.31E-01	0.32E-01
PHASE	-142.	73.	107.	-86.	105.	-88.	93.
7. 5							
4P MAG	0.10E-01	0.64E-02	0.92E-02	0.10E-01	0.16E-01	0.49E-02	0.79E-02
PHASE	-122.	117.	173.	-11.	-54.	120.	-72.
7. 6							
4P MAG	0.18E-01	0.15E-01	0.17E-01	0.70E-01	0.20E-01	0.61E-02	0.85E-02
PHASE	142.	1.	45.	-139.	161.	-4.	154.
7. 4							
4P MAG	0.49E-02	0.46E-02	0.36E-02	0.27E-02	0.84E-02	0.20E-02	0.46E-02
PHASE	175.	8.	82.	-103.	26.	-168.	47.

RUN.PT	CHANNEL DESIGNATION						
	1	2	3	4	5	6	7
7. 3							
4P MAG	0.16E-01	0.10E-01	0.15E-01	0.17E-01	0.21E-01	0.85E-02	0.82E-02
PHASE	55.	-90.	-15.	172.	173.	-21.	166.
6. 6							
4P MAG	0.49E-01	0.32E-01	0.16E-01	0.14E-01	0.24E-01	0.56E-02	0.58E-02
PHASE	113.	-65.	23.	-155.	-30.	106.	-27.
6. 5							
4P MAG	0.44E-01	0.30E-01	0.15E-01	0.16E-01	0.56E-02	0.55E-02	0.21E-02
PHASE	-111.	79.	165.	-17.	122.	-156.	54.
6. 3							
4P MAG	0.63E-02	0.80E-02	0.10E-01	0.13E-01	0.92E-01	0.19E-01	0.17E-01
PHASE	-165.	-49.	-51.	168.	-179.	-20.	164.
6. 4							
4P MAG	0.67E-01	0.27E-01	0.22E-01	0.36E-01	0.58E-01	0.14E-01	0.11E-01
PHASE	129.	-37.	77.	-103.	-150.	49.	-148.
8. 7							
4P MAG	0.27E-01	0.11E-01	0.10E-01	0.10E-01	0.21E-01	0.33E-02	0.91E-02
PHASE	-45.	151.	-121.	30.	-70.	118.	-84.
8. 6							
4P MAG	0.70E-01	0.19E-01	0.25E-01	0.20E-01	0.21E-01	0.30E-02	0.93E-02
PHASE	46.	-127.	2.	-167.	-59.	20.	-43.
8. 5							
4P MAG	0.13E-01	0.63E-02	0.10E-02	0.57E-02	0.20E-01	0.21E-02	0.50E-02
PHASE	143.	-82.	148.	-39.	25.	114.	-42.
7. 7							
4P MAG	0.82E-01	0.31E-01	0.27E-01	0.31E-01	0.84E-01	0.78E-02	0.38E-02
PHASE	92.	-85.	23.	-150.	-162.	-8.	109.

RUN.PT		CHANNEL DESIGNATION						
		1	2	3	4	5	6	7
8. 4								
4P	MAG	0.22E+00	0.67E-01	0.37E-01	0.11E-01	0.13E+00	0.27E-01	0.72E-01
	PHASE	43.	-131.	7.	-124.	177.	-178.	6.
7. 9								
4P	MAG	0.16E+00	0.72E-01	0.54E-01	0.59E-01	0.53E-01	0.21E-01	0.43E-01
	PHASE	25.	-143.	-37.	163.	119.	18.	-106.
7. 8								
4P	MAG	0.11E+00	0.44E-01	0.37E-01	0.28E-01	0.86E-01	0.78E-02	0.29E-01
	PHASE	-23.	179.	-59.	147.	148.	34.	-91.
10. 7								
4P	MAG	0.45E-01	0.12E-01	0.68E-02	0.13E-01	0.21E-01	0.48E-02	0.37E-02
	PHASE	-29.	129.	-116.	28.	-26.	-100.	115.
10. 6								
4P	MAG	0.42E-01	0.13E-01	0.12E-01	0.17E-01	0.37E-01	0.77E-02	0.20E-01
	PHASE	-5.	146.	-87.	92.	73.	21.	-129.
8. 9								
4P	MAG	0.11E+00	0.61E-01	0.98E-02	0.18E-01	0.60E-01	0.74E-02	0.17E-01
	PHASE	174.	-31.	59.	-77.	-58.	-19.	126.
10. 5								
4P	MAG	0.67E-01	0.21E-01	0.77E-02	0.13E-01	0.70E-01	0.19E-01	0.41E-01
	PHASE	-76.	100.	-105.	-177.	124.	85.	-95.
8. 8								
4P	MAG	0.33E-01	0.14E-01	0.13E-01	0.35E-01	0.10E+00	0.14E-01	0.30E-01
	PHASE	104.	-104.	16.	-153.	179.	155.	-15.
9. 7								
4P	MAG	0.34E-01	0.18E-01	0.32E-02	0.10E-01	0.54E-01	0.25E-01	0.47E-01
	PHASE	151.	-7.	-120.	37.	-67.	-58.	125.

RUN.PT		CHANNEL DESIGNATION					
	1	2	3	4	5	6	7
9. 6							
4P MAG	0.46E-01	0.34E-02	0.22E-02	0.24E-01	0.65E-01	0.18E-01	0.41E-01
PHASE	170.	-87.	-57.	-148.	157.	84.	-93.
9. 5							
4P MAG	0.26E+00	0.10E+00	0.11E-01	0.22E-01	0.24E-01	0.18E-02	0.25E-01
PHASE	95.	-111.	4.	130.	-173.	-140.	22.
9. 4							
4P MAG	0.23E+00	0.10E+00	0.24E-01	0.44E-01	0.94E-01	0.22E-01	0.60E-01
PHASE	128.	-78.	-8.	-177.	-178.	148.	-8.
9. 3							
4P MAG	0.65E-01	0.84E-02	0.56E-02	0.28E-01	0.37E-01	0.24E-01	0.50E-01
PHASE	43.	-97.	27.	41.	-81.	-125.	60.

REFERENCES

1. Staley, J. A.: Validation of Rotorcraft Flight Simulation Program Through Correlation with Flight Data for Soft Inplane Hingeless Rotors. USAAMRDL TR 75-50, Jan. 1976.

2. Dixon, P. G. C.: Design, Development, and Flight Demonstration of the Loads and Stability Characteristics of a Bearingless Main Rotor. USAAVRADCOM TR-80-D-3, 1980.

3. Hammond, C. E.; and Doggett, R.: Demonstration of Subcritical Damping by Moving Block/Randomdec Applications. NASA SP-415, 1976, pp. 59-76.

TABLE 1.- DESCRIPTION OF BO-105 ROTOR

Item	Specification
Type	Hingeless
Rotor radius (m)	4.91
Number of blades	4
Blade chord (m)	0.27
Linear blade twist (deg)	-8.0
Solidity, σ	0.07
Reference area, S(m^2)	5.30
Airfoil section	NACA 23012
Hub height above floor (m)	6.89
Shaft angle of attack (deg)	-10.0

TABLE 2.- CALCULATED ROTATING BLADE FREQUENCIES (per rev) AT 425 rpm

	First mode	Second mode	Third mode
Flapwise	1.12	2.76	5.06
Edgewise	0.70	4.30	-
Torsion	3.19	-	-

TABLE 3.- SUPPORT SYSTEM DYNAMIC CHARACTERISTICS FOR BO-105 HOVER TEST

Direction of excitation	Mode	ω, Hz	C_ζ, N-S/M
Longitudinal	Balance	2.24	119,600
	Strut	4.17	49,160
Lateral	Balance	2.71	51,900
	Strut	4.64	35,940

TABLE 4.- ROTOR INSTRUMENTATION

	Blade No.	Station	Units	Positive sign convention
Blade				
Chord bending	1	0.10R	N-m	Leading edge in tension
	3	0.10R	N-m	
	1	0.57R	N-m	
Flap bending	1	0.10R	N-m	Flapping up
	1	0.28R	N-m	
	1	0.57R	N-m	
	1	0.80R	N-m	
Torsion	1	0.34R	N-m	Leading edge up
Pitch link	1	--	N	Tension
Rotor shaft torque	--	--	N-m	Direction of rotation

TABLE 5.- ROTOR TEST APPARATUS ACCELEROMETERS

Location in RTA	Channel	Direction	Units
Nose	1	Vertical	g's
Transmission	2	Longitudinal	g's
Tail	3	Longitudinal	g's
Right side	4	Longitudinal	g's
Tail	5	Lateral	g's
Left side	6	Lateral	g's
Right side	7	Lateral	g's

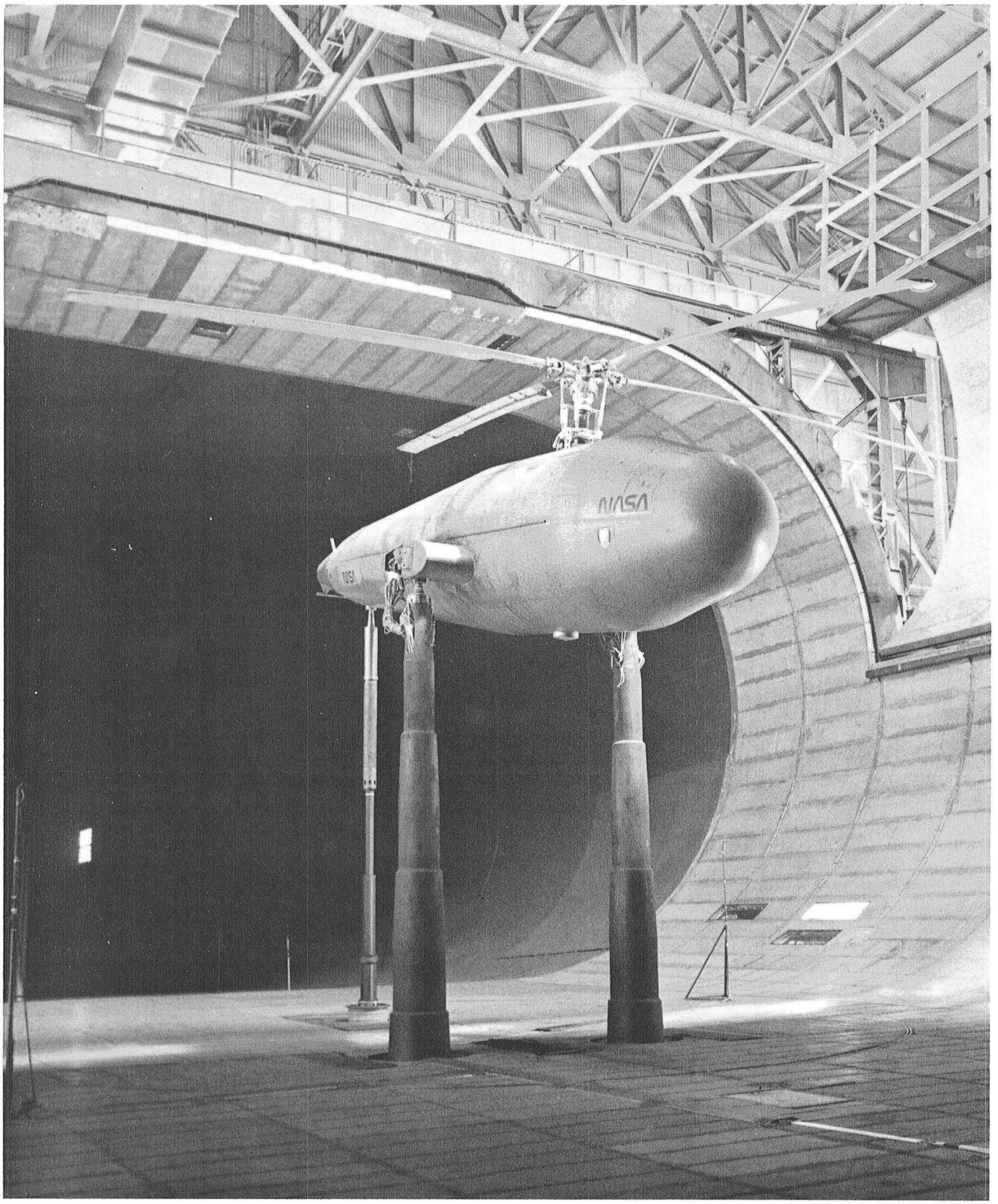

Figure 1.- BO-105 rotor system on Ames rotor test apparatus in 40- by 80-Foot Wind Tunnel Test Section

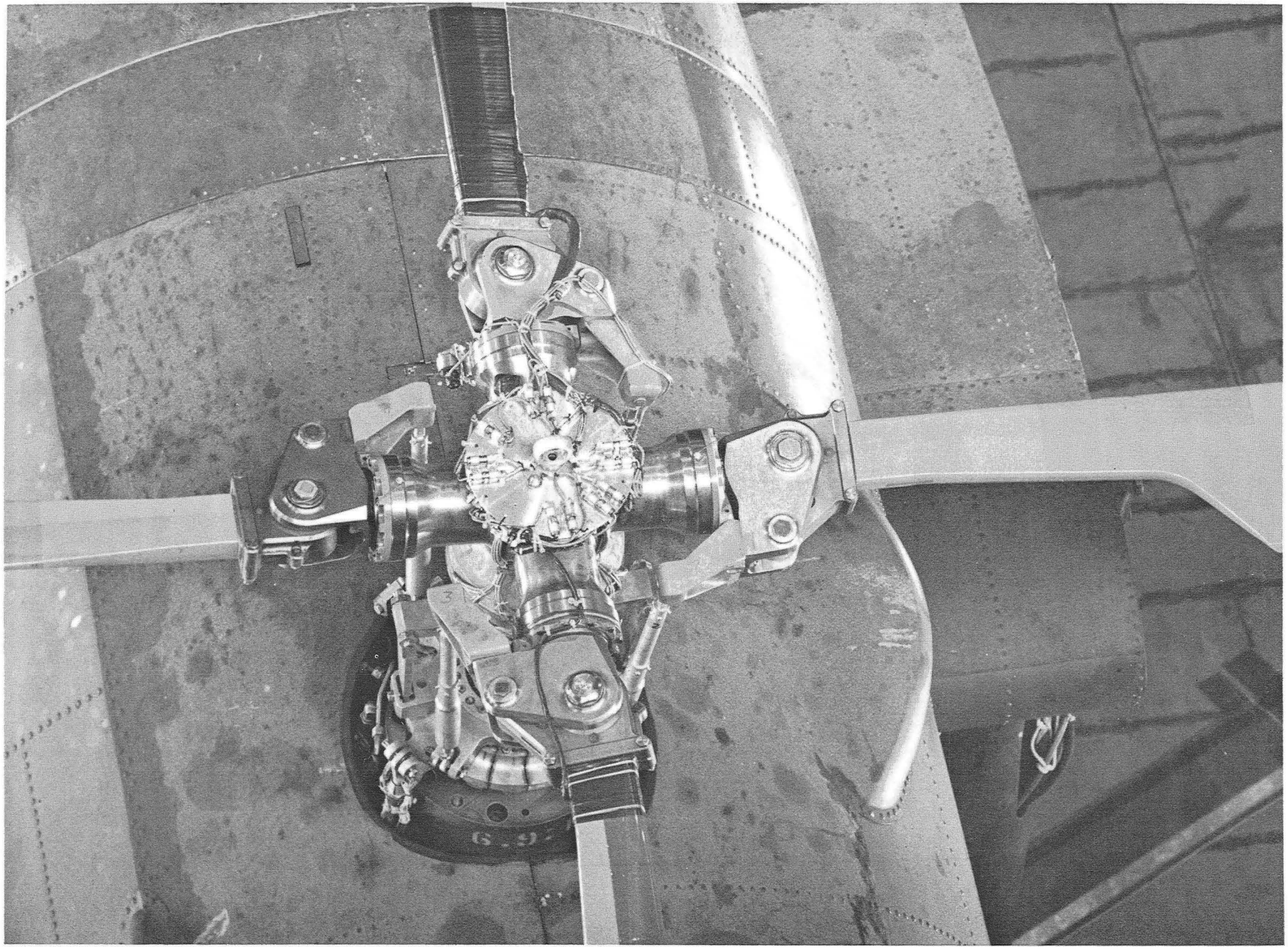

Figure 2.- BO-105 hingeless rotor hub.

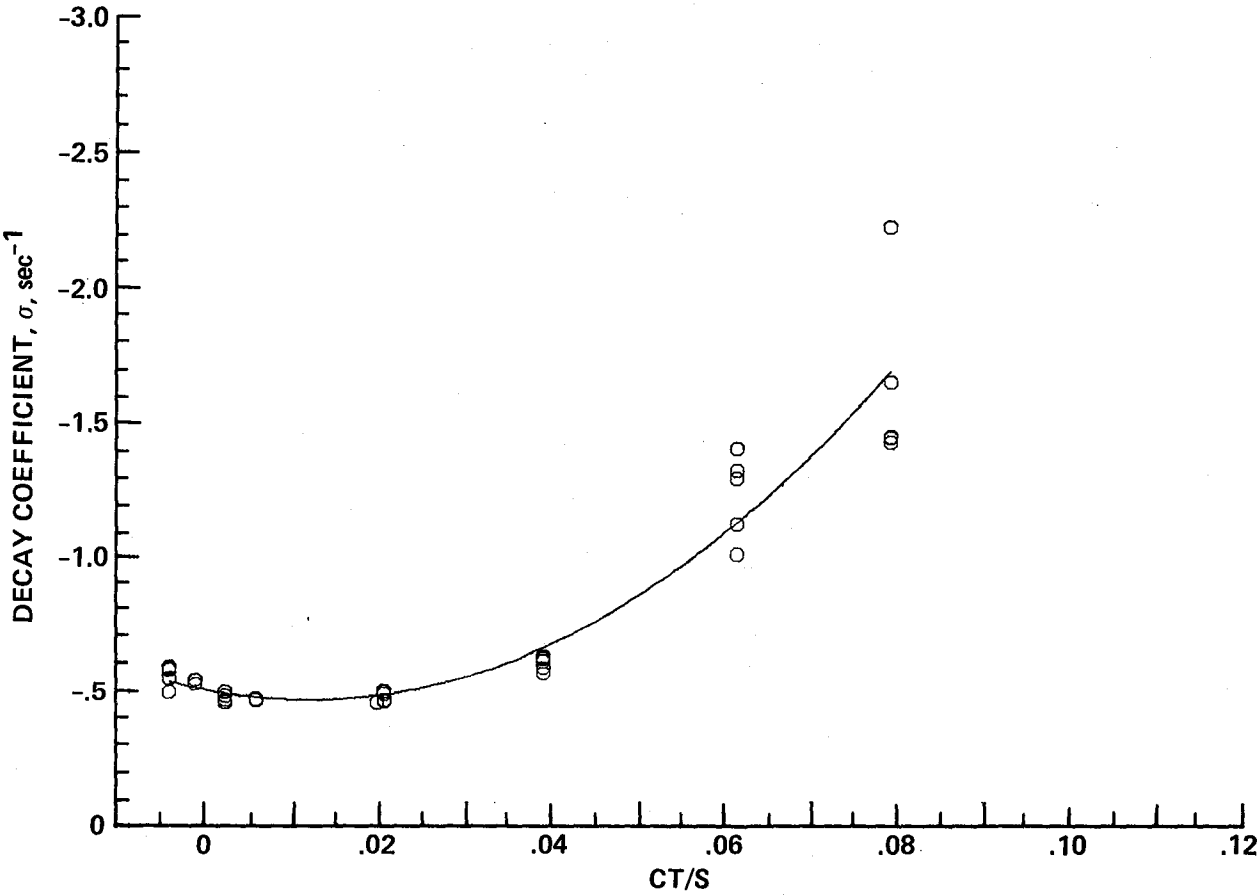

Figure 3.- Decay coefficient, σ (sec^{-1}) vs C_T/σ, 350 rpm.

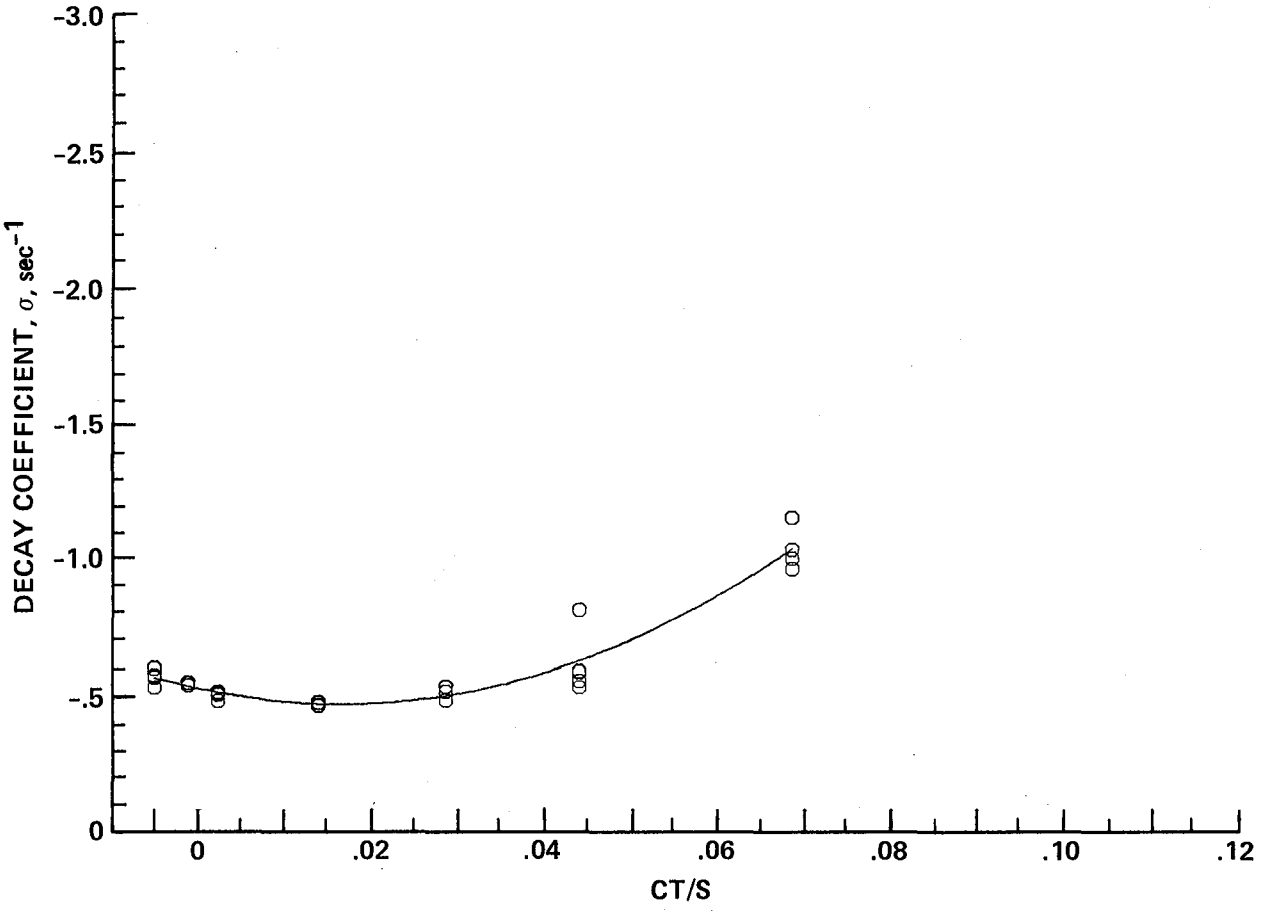

Figure 4.- Decay coefficient, σ (sec^{-1}) vs C_T/σ, 375 rpm.

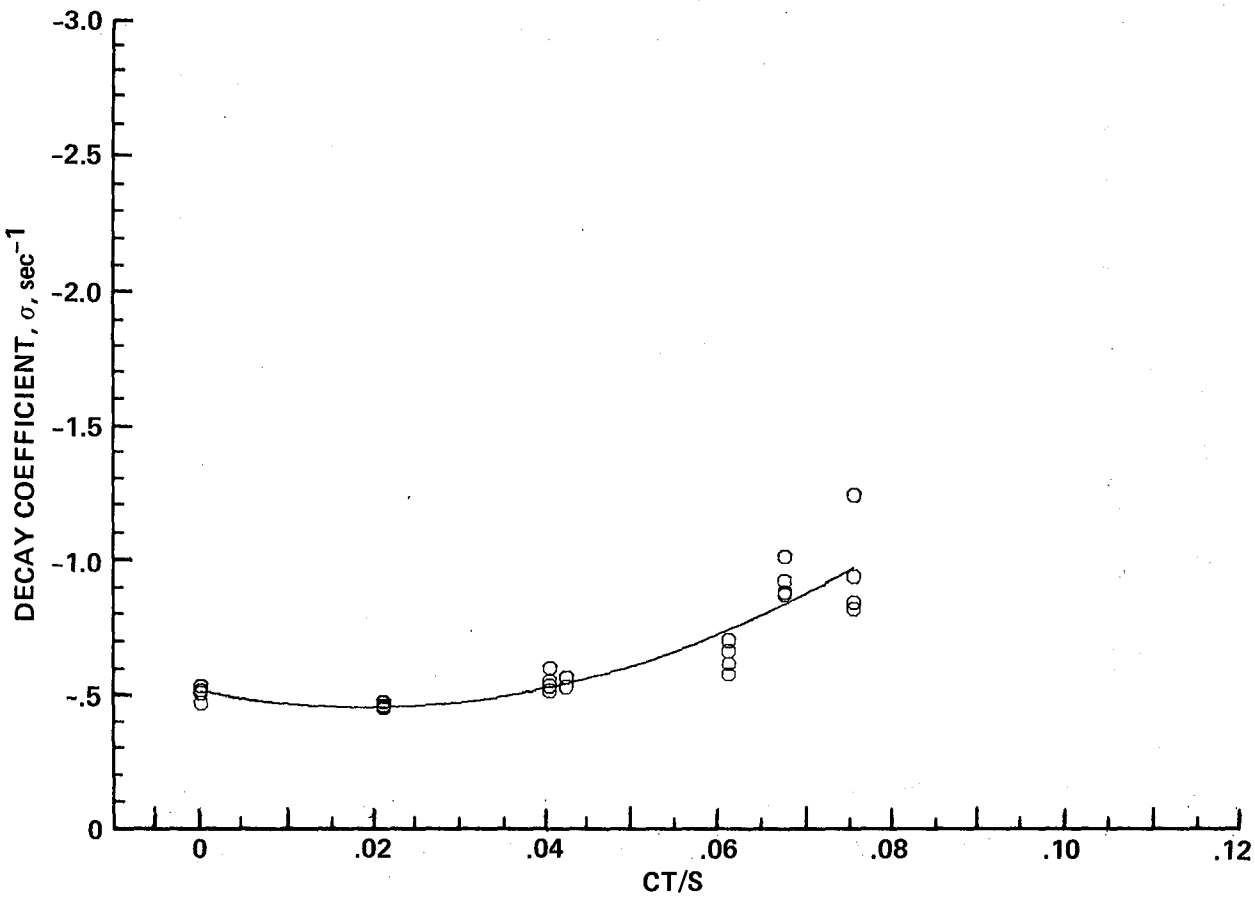

Figure 5.- Decay coefficient, σ (sec^{-1}) vs C_T/σ, 400 rpm.

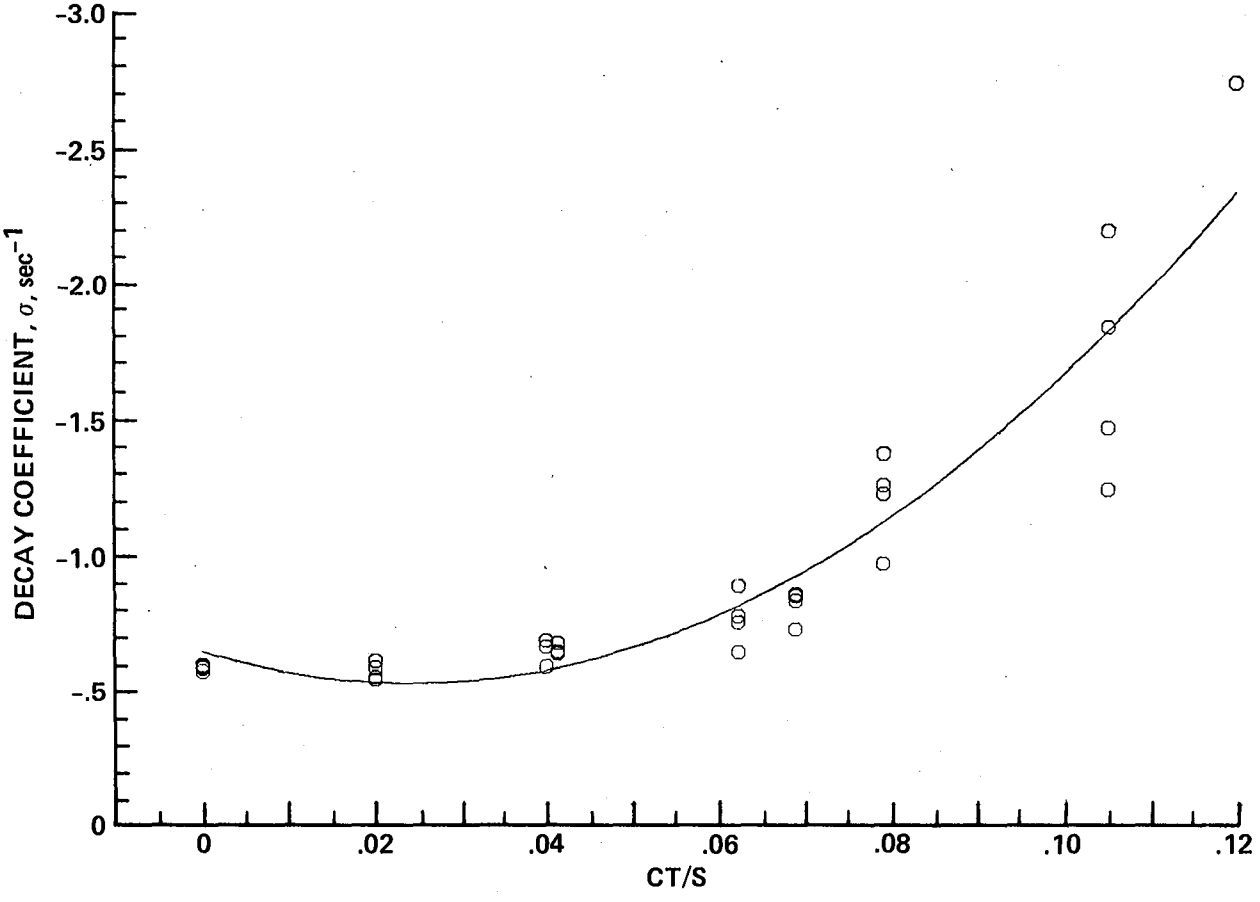

Figure 6.- Decay coefficient, σ (sec^{-1}) vs C_T/σ, 425 rpm.

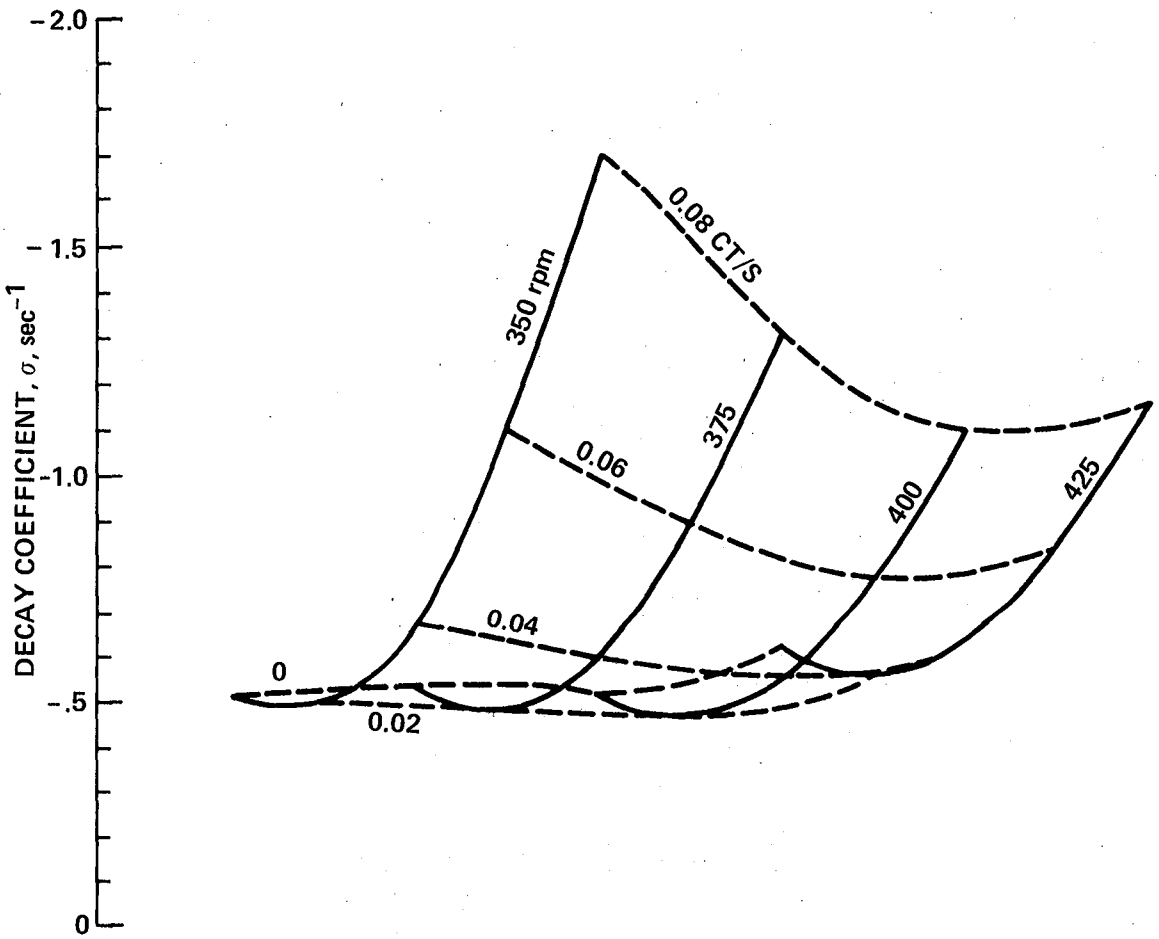

Figure 7.- Curve-fit hover stability data.

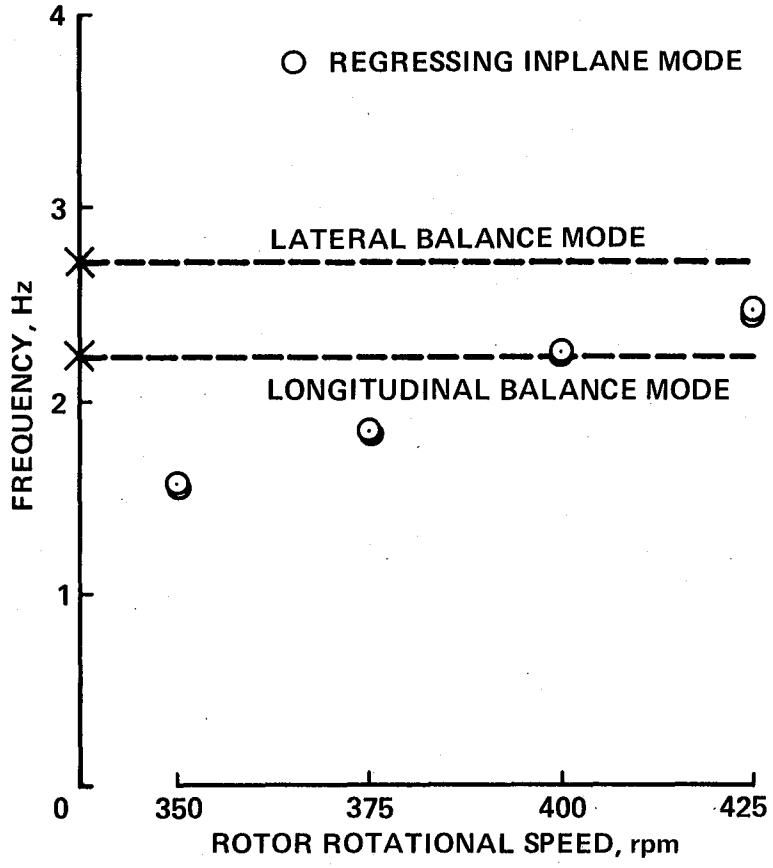

Figure 8.- Inplane regressing mode frequency (Hz) as a function of rotor rotational speed (C_T/σ = 0.07).

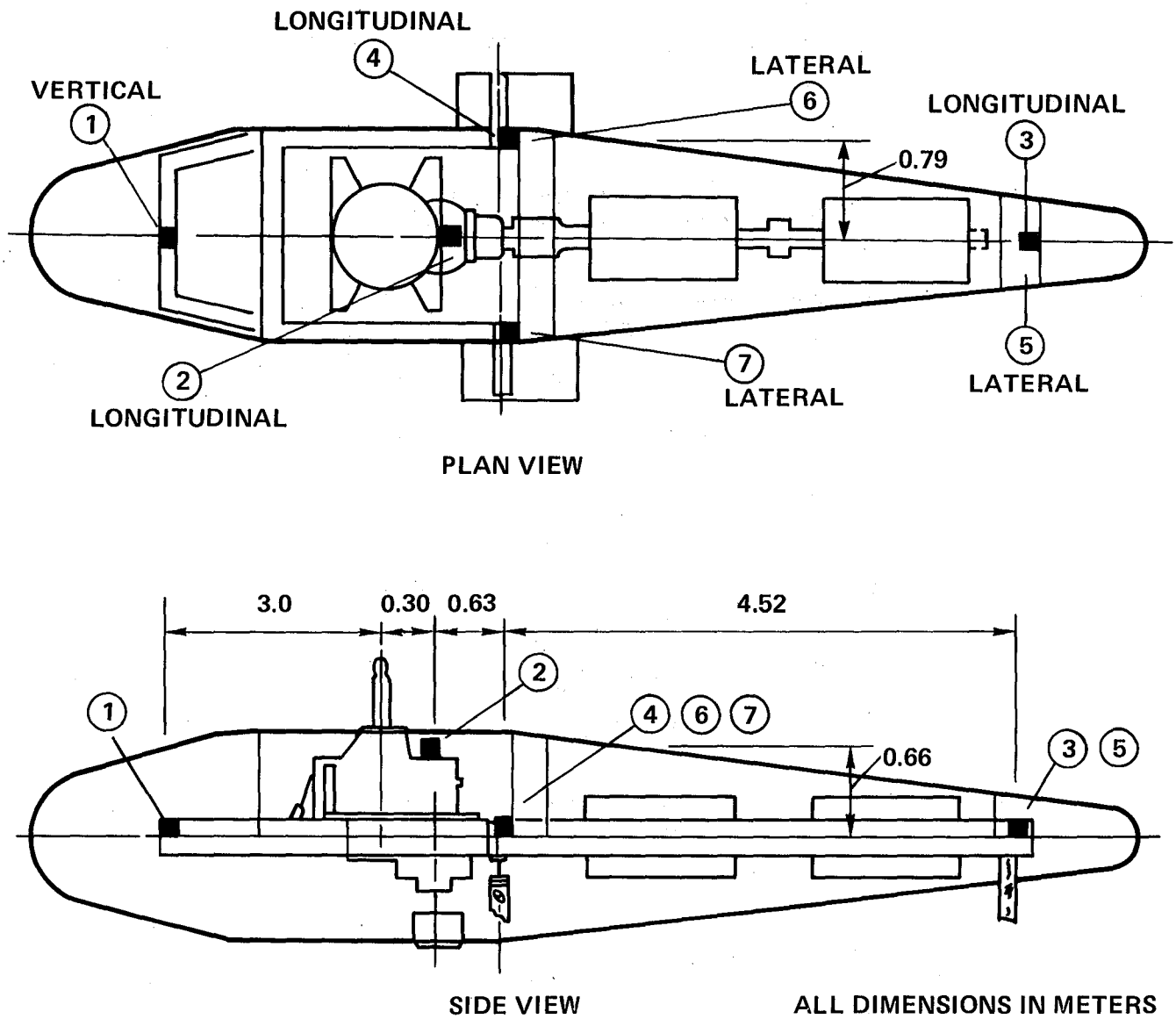

Figure 9.- Location of accelerometers on rotor test apparatus.

1. Report No. NASA TM 84892	2. Government Accession No.	3. Recipient's Catalog No.
4. Title and Subtitle HOVER TEST OF A FULL-SCALE HINGELESS HELICOPTER ROTOR: AEROELASTIC STABILITY, PERFORMANCE, AND LOADS DATA		5. Report Date January 1984 6. Performing Organization Code
7. Author(s) Randall L. Peterson and William Warmbrodt		8. Performing Organization Report No. A-9573 10. Work Unit No. T-3504
9. Performing Organization Name and Address Ames Research Center Moffett Field, CA 94035		11. Contract or Grant No. 13. Type of Report and Period Covered Technical Memorandum
12. Sponsoring Agency Name and Address National Aeronautics and Space Administration Washington, D.C. 20546		14. Sponsoring Agency Code 532-06-11

15. Supplementary Notes Point of Contact: R. Peterson, Ames Research Center, MS 247-1, Moffett Field, CA 94035 (415) 965-5044 or FTS 448-5044

16. Abstract

A hover test of a full-scale, hingeless rotor system was conducted in the NASA Ames 40- by 80-Foot Wind Tunnel. The rotor was tested on the Ames Rotor Test Apparatus (RTA). Rotor aeroelastic stability, performance, and loads at various rotational speeds and thrust coefficients were investigated. The primary objective was to determine the inplane stability characteristics of the rotor system. Rotor inplane damping data were obtained for operation between 350 and 425 rpm (design speed), and for thrust coefficients (C_T/σ) between 0.0 and 0.12. The rotor was stable for all conditions tested. At constant rotor rotational speed, a minimum inplane damping level was obtained at approximately $C_T/\sigma = 0.02$. At constant rotor lift, a minimum in rotor inplane damping was measured at 400 rpm.

17. Key Words (Suggested by Author(s))	18. Distribution Statement
Helicopter design Rotary wing Dynamic stability	Unlimited Subject Category - 05

19. Security Classif. (of this report)	20. Security Classif. (of this page)	21. No. of Pages	22. Price*
Unclassified	Unclassified	54	A02

*For sale by the National Technical Information Service, Springfield, Virginia 22161